

Shake Table Tests: Seismic Performance of Anchors Connecting Suspended Nonstructural Components to Concrete



P. Mahrenholtz

University of Stuttgart, Germany

T. C. Hutchinson

University of California, San Diego, USA

R. Eligehausen & J. Hofmann

University of Stuttgart, Germany

SUMMARY

Robust earthquake resistant connections are important to avoid substantial damage to nonstructural components and systems (NCS) and to limit costs associated with failure or loss of functionality of the NCS. Suspended NCSs are particularly noted for rendering excessive downtime in past earthquakes. In order to deepen the understanding of the seismic performance of post-installed concrete anchors supporting suspended NCS, shake table tests were conducted on anchors connecting a suspended model component to a cyclically cracked concrete slab. The concrete slab was subjected to seismic floor accelerations and corresponding floor level cyclic crack width histories to simulate the boundary conditions anticipated in floors of a building during an earthquake. Undercut anchors and expansion anchors were tested using an incremental dynamic approach to failure. The suspended single mass model component replicated typical oscillation period of NCS. This paper focuses on the load transfer and failure mechanisms and presents test data that illustrate key anchor performance characteristics.

Keywords: Shake table, Nonstructural components, Experimental earthquake simulation, Seismic performance, Post-installed anchors

1. INTRODUCTION

Concrete anchors are used to connect structural elements with each other, i.e. structural connections, or to fix components, in particular the non-load bearing components of a structure, to the primary structure, i.e. nonstructural connections. Due to the flexibility, easy handling, and large field of possible applications, post-installed anchors have clear advantages over cast-in-place anchors and thus are increasingly popular among designers and contractors. Nonstructural connections represent a large portion of the seismic relevant application of post-installed anchors. Termed NCS, these nonstructural components and systems may be broadly categorised as mechanical-electrical-plumbing (MEP), architectural, or contents (*ASCE 7 (2010)*). Many NCSs are not considered in the seismic design process, and none are utilised as the primary load carrying system of a building.

Because of the stress concentration present at the anchor holes and the weakening of the cross section, the probability is high that anchor positions are transected by cracks (e.g. *Eligehausen et al. (1986)*; *Bergmeister (1988)*). Since cracks have a negative influence on the anchor performance, the assumption that anchors are generally situated in a crack is conservative. As the structure responds to an earthquake motion, it deforms, and the cracks open and close cyclically. The oscillating structure serves as a filter and amplifies the ground acceleration a_g near the natural frequencies of the structure. The characteristics of the resulting floor accelerations a_{floor} depend not only on the input motion, but importantly on the specific building design and in particular its height as well as the floor level considered (e.g. *Paulay and Priestley (1992)*, *Bachmann (2002)*).

For nonstructural connections, the anchor loads develop due to the inertial response of the component to the acceleration of the floor it is connected to. As a result of the primary structural component oscillation and the secondary component oscillation, any given seismic event causes cycling of anchor

loads and crack widths simultaneously. The resulting anchor response in turn feeds back the behaviour of the anchored component.

The seismic performance of nonstructural components and their anchorage have been neglected for a long time despite the fact that damage to them has been shown to cause substantial economic loss and pose a considerable risk to life safety. Moreover, nonstructural components generally form the major portion of the total building investment costs and therefore represent large potential financial losses (e.g. *Herdman (1995), Taghavi and Mirand. (2003), Schuler (2007)*). Vulnerable components may be rendered inoperable even at low displacement demands and are not available when they are needed most, e.g. medical equipment in hospitals, or cause consecutive hazards, e.g. safety relevant piping systems in nuclear power plants. Sufficient and suitable anchorage is therefore essential.

To investigate the seismic response of post-installed anchors on system level, shake table tests were conducted at the University of California, San Diego as part of an international research project on seismic performance of anchors. The tests were carried out on anchors connecting a suspended model component to a concrete slab representing a structural component in a building. The component was subjected to floor accelerations, and simultaneously the cracks in the concrete were opened and closed cyclically. The floor acceleration and corresponding floor level cyclic crack width histories were based on nonlinear simulations of representative reinforced concrete structures responding to real earthquake records. The test program included several test suites investigating different aspects. This paper presents the failure tests for which the anchored component was incrementally loaded to failure. The tests facilitated understanding of the complex load transfer mechanism and identification of the driving performance parameters.

2. EXPERIMENTAL APPROACH AND PROCEDURES

2.1. Testing Approach and Test Setup

Anchors in nonstructural connections are loaded according to the inertial response of the anchored component to the floor acceleration. The seismic demand acting on the anchorage is the result of the supporting floor acceleration, whereas the capacity of the anchor as well as its demand are affected by the concrete cracking histories. This in turn is also influenced by the anchor behaviour in response to the loading. The complex interaction of component and anchor responding to floor acceleration and cracking warrants investigation via full-scale shake table tests. As the anchors are additionally loaded by gravity loads, suspended installations are more critical than floor mounted installations. Therefore, the shake table tests presented in the following were conducted on a suspended model component, which was connected to the soffit of a model concrete slab (Fig. 2.1).

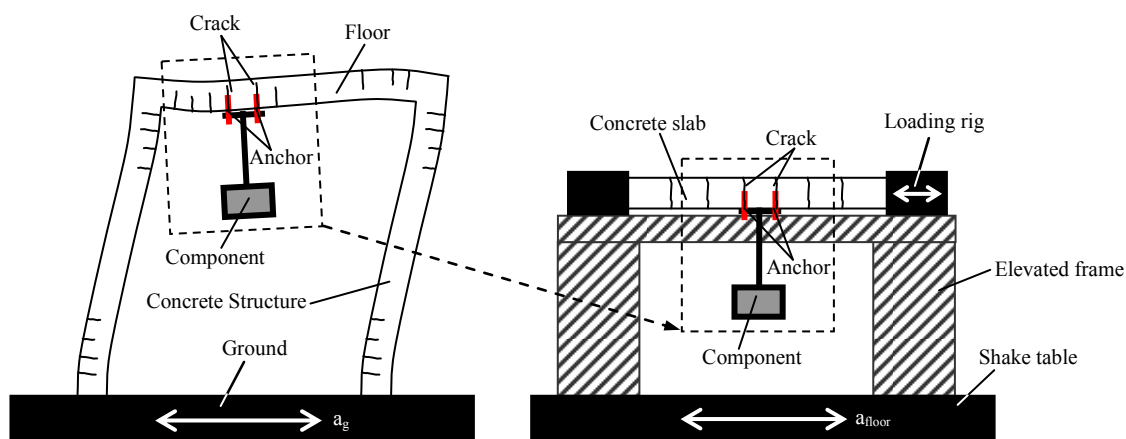


Figure 2.1. Component connected to real structure (left) and to model concrete component mounted in loading rig on shake table (right)

The model slab may represent any type of concrete component (e.g. beam or slab) that a nonstructural component could be anchored to. The test setup mimicked the floor acceleration and corresponding crack behaviour at that particular location. Fig. 2.2 shows a picture of the test setup. The main elements of the test setup are the shake table (1), an elevated steel frame (2), the loading rig including actuators (3), the model concrete slab (4) and the model component (5). The total mass of the elevated test setup summed up to 8750 kg. The total height of the elevated test assembly was nearly 3 m. The single axis shake table has a platen dimension of 3050 x 4875 mm and is operated by a single, double acting actuator with a nominal capacity of 445 kN allowing a maximal acceleration of the unloaded table of 9 g. The peak velocity attainable is 880 mm/s and the maximum displacement attainable ± 330 mm. The table is controlled by an accelerometer installed underneath the platen.

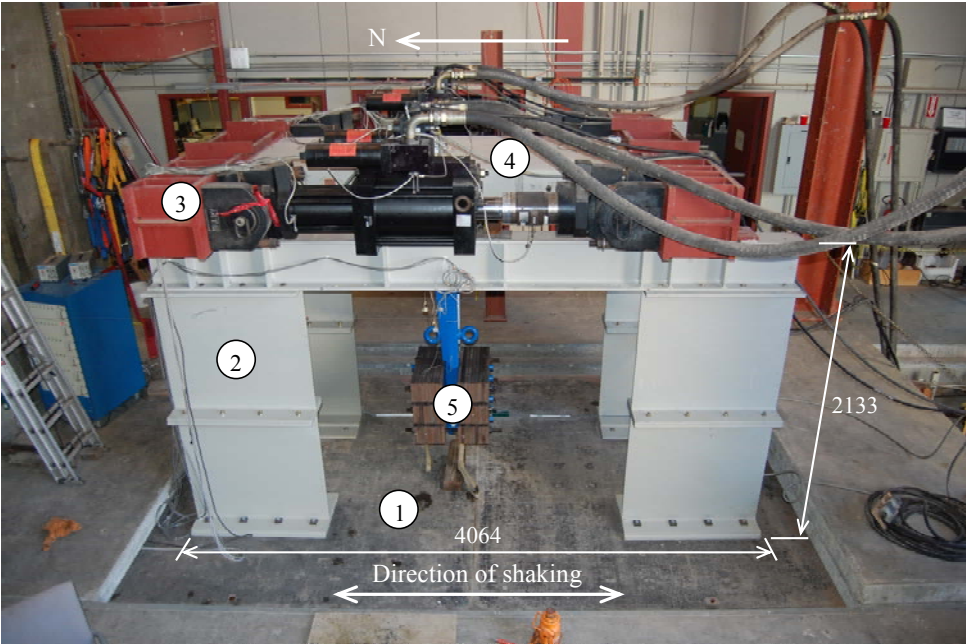


Figure 2.2. Picture of test setup (all units in mm)

The model component had four footings, which were fixed to the model concrete slab by means of post-installed anchors (Fig. 2.3a). The total weight of the component was 11.3 kN and the corresponding natural period of vibration was 0.25 seconds. The loading rig (Fig. 2.3b) consisted basically of two head beams, to which the concrete slab was attached to, coupled with a pair of servo hydraulic actuators (735 kN) used to open and close the cracks in the concrete slab dynamically.

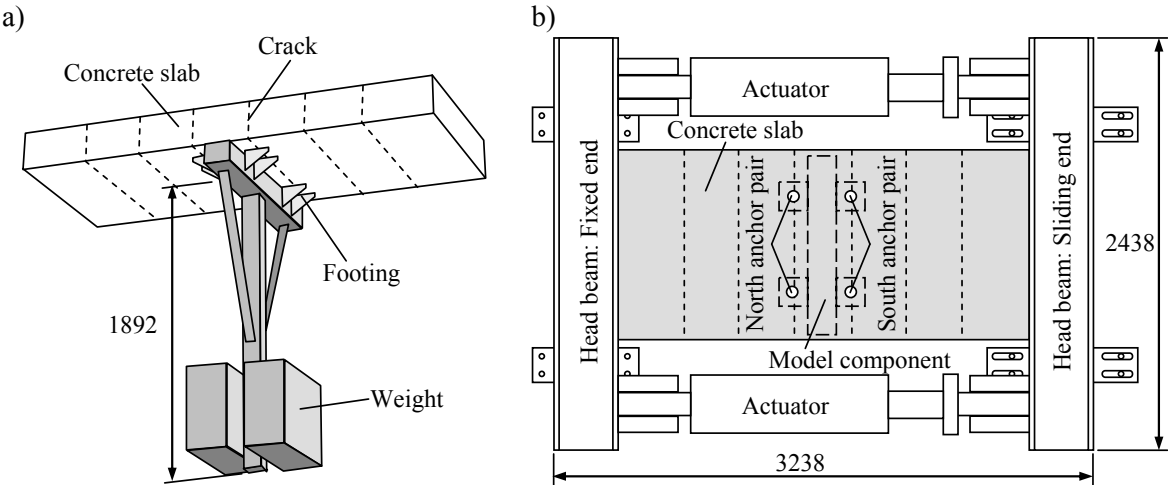


Figure 2.3. a) Isometric view of model component connected to concrete slab; b) Plan view of loading rig with mounted concrete slab (all units in mm)

The head beams were mounted on the two longitudinal beams of the elevated frame. One head beam was permanently fixed, while the other rested on sliding plates allowing free movement in the longitudinal direction. A detailed description of the model component and loading rig is available in *Watkins and Hutchinson (2011)*.

The floor acceleration and crack width time histories used in this test program are based on non-linear analyses presented in *Wood et al. (2010)*, and simulate the response of the 1st floor of a 2-story building subjected to a motion from the 1995 Kobe Earthquake. The resulting peak floor acceleration was 0.950 g. A linear relationship between curvature and crack width was assumed. Fig. 2.4 plots the normalised time histories for floor acceleration and crack width. In this case the acceleration is normalised by the peak floor acceleration (PFA) and the crack width is normalised by the maximum crack width.

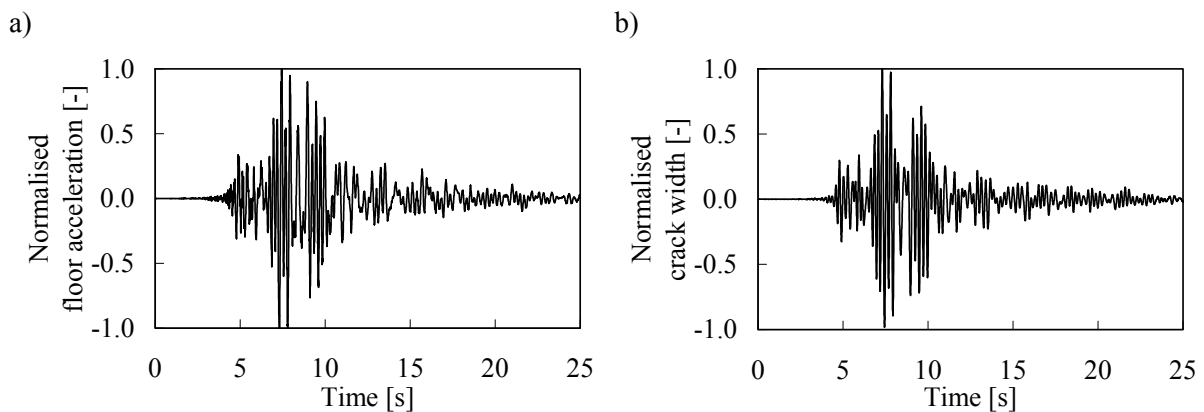


Figure 2.4. Normalised time histories for a) floor acceleration and b) crack width

The anchor load develops according to the response of the anchored model component to the acceleration and the cycling cracks in the concrete slab. By scaling the floor acceleration and crack width time histories, the maximum anchor load and crack width, respectively, can be controlled.

The response of the model component and anchors was measured by various sensors, namely displacement transducers, load cells and accelerometers. In addition, information was collected from the shake table and loading rig actuators, including the displacement, velocity, and acceleration, to control floor acceleration and cracking. The strain in the concrete slab reinforcement was monitored using strain gauges. In total, 84 data acquisition channels recorded information at a sampling rate of 200 Hz. The most important measurements included crack widths at the anchor locations, system, floor, and component accelerations, and anchor axial loads and displacements. In addition an array of video cameras was used to capture the physical development of damage at the anchors and the global response of the suspended component. Test videos containing three camera views and synchronised test data plots were produced. The shown data included the table acceleration and displacement, the averaged crack width for the north and south anchor pairs, as well as the loads and displacements of all anchors.

2.2. Anchors and Concrete

Two types of post-installed anchors were tested (Fig. 2.5a): One undercut anchor M10, which is relatively insensitive to large cracks, and one torque-controlled expansion anchor, bolt-type, 1/2", which is relatively sensitive to large cracks. The expansion anchor consists of a bolt with a conical end and expansion elements, which are expanded and pressed against the borehole wall during installation. The anchor load is then transferred to the concrete by friction. The load transfer mechanism of the undercut anchor is provided by mechanical interlock between the anchor and the concrete. This interlock is created by a special installation procedure that facilitates the anchor cutting itself into the

borehole walls. Both anchor products were prequalified for seismic loads according to *ACI 355.2 (2007)*.

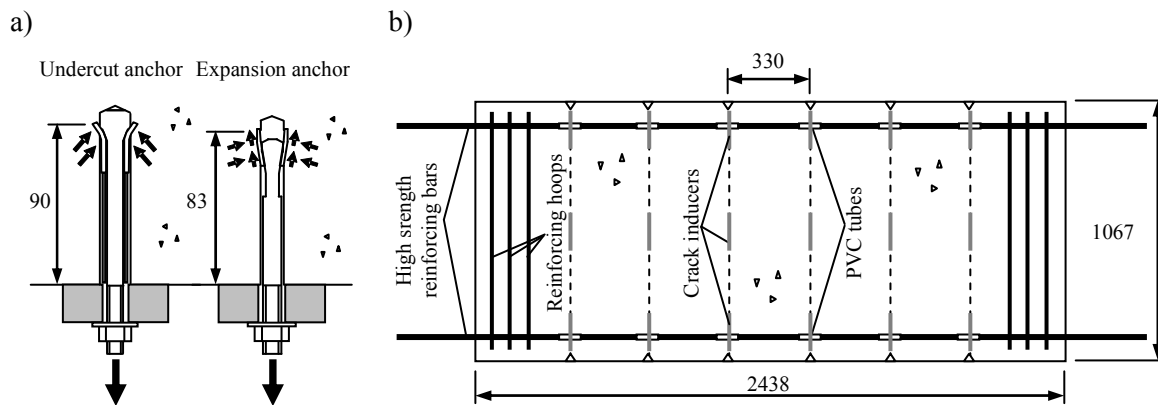


Figure 2.5. a) Post-installed anchor types considered in this study; b) Geometry, reinforcement and details of model concrete slabs (all units in mm)

The 254 mm thick model reinforced concrete slabs (Fig. 2.5b) were made of low strength concrete with a nominal concrete compressive strength of $f_c = 25$ MPa. The longitudinal reinforcement of the slabs consisted of four 22 mm high strength reinforcing bars. Three 19 mm reinforcing hoops were placed at the ends of the slab for confinement. The slabs were detailed to crack at 330 mm spacing using 3 mm thick stainless steel sheet metal crack inducers installed prior to concrete pour. To ensure that the crack runs through the thickness of the slab and straight, pilot holes were drilled prior to crack initialisation. For increased assurance of crack generation at the target locations, the longitudinal reinforcement was debonded around the envisaged crack positions using 100 mm long PVC tubes.

2.3. Test Objectives and Program

The primary goal of the tests was to investigate the failure mechanism and ultimate capacity of the anchors, thereby loading the anchors beyond the load level they are qualified for. Testing of undercut and expansion anchor types with different load-displacement characteristics allowed investigating the impact of different anchor types on the performance. The crack width time histories were scaled to a peak crack width of 0.8 mm associated with the maximum possible crack width outside of plastic hinges (*Hoehler (2006)*). Using an incremental dynamic analysis approach allowed testing one anchored model component at various demand levels before it finally achieves failure. Therefore, the anchors were not designed for a certain degree of utilisation but the amplitude scale factor was incrementally increased after each test run until the anchorage finally failed. In total, 7 test runs were conducted for the component anchored by undercut and expansion anchors. The test program and key test parameters are given in Table 2.1. It is noted that the undercut anchor failed at a motion scale twice that of the expansion anchor (130 % versus 60 %).

Table 2.1. Test Program and Key Test Parameters

| Anchor type | No. of tests | Maximum floor acceleration (at 100 %) | Amplitude scaling | Maximum crack width |
|------------------|--------------|---------------------------------------|--------------------|---------------------|
| Undercut anchor | 4 | 0.95 g | 40, 70, 100, 130 % | 0.8 mm |
| Expansion anchor | 3 | 0.95 g | 20, 40, 60 % | 0.8 mm |

3. EXPERIMENTAL RESULTS AND DISCUSSION

3.1. General Behaviour and Load-Transfer Mechanism

During shaking, the model component is accelerated and its mass inertia results in alternate loading of the north and south anchor pairs. At any instant in time, one pair is in tension while the other may be

unloaded (Fig. 3.1a). Though the magnitudes of the individual anchor loads differ to a certain degree, the two anchors of a pair are principally loaded at the same time. The loading generates anchor displacement in particular when the crack intersecting the anchor location is opened and therefore the stiffness of the anchor is decreased. The rotation of the model component around the footing contacting the concrete slab increases with increasing load amplitudes. Due to the anchor displacement, the model component becomes loose and does not oscillate in its original period of 0.25 seconds but experience a period elongation. The spectral acceleration shows the peak at an elongated period (Fig. 3.1b).

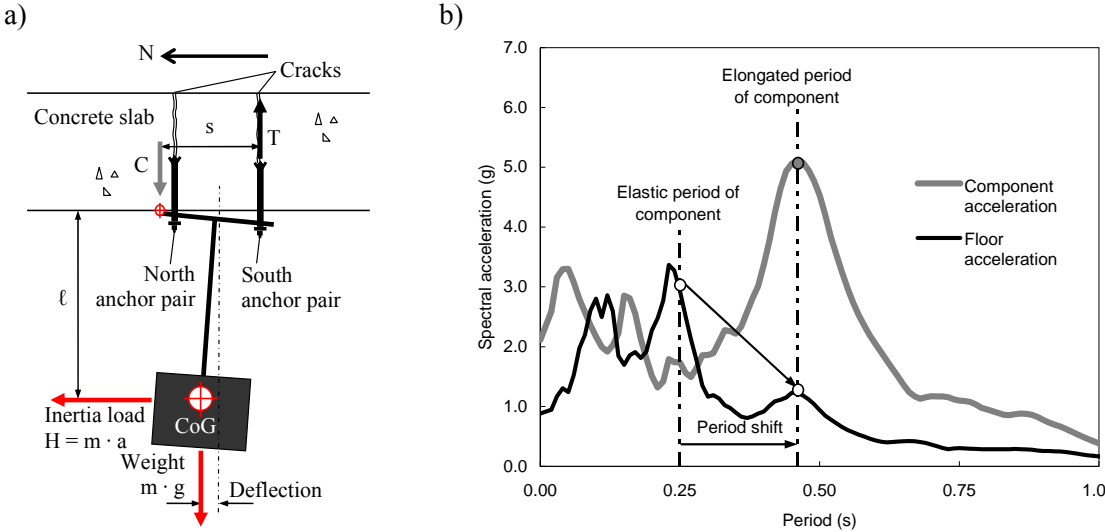


Figure 3.1. a) Schematic load transfer mechanism; b) Elastic acceleration spectra of the measured floor and component accelerations (example: Undercut anchor, 40% scaling)

Plotting the axial loads of the north and south anchor pairs (Fig. 3.2) illustrates the alternate loading, which develops correspondingly to the deflection of the model component measured at the centre of gravity (CoG). The time histories show a relatively constant oscillation. The corresponding period matches with the peak of the component response spectrum (Fig. 3.1b).

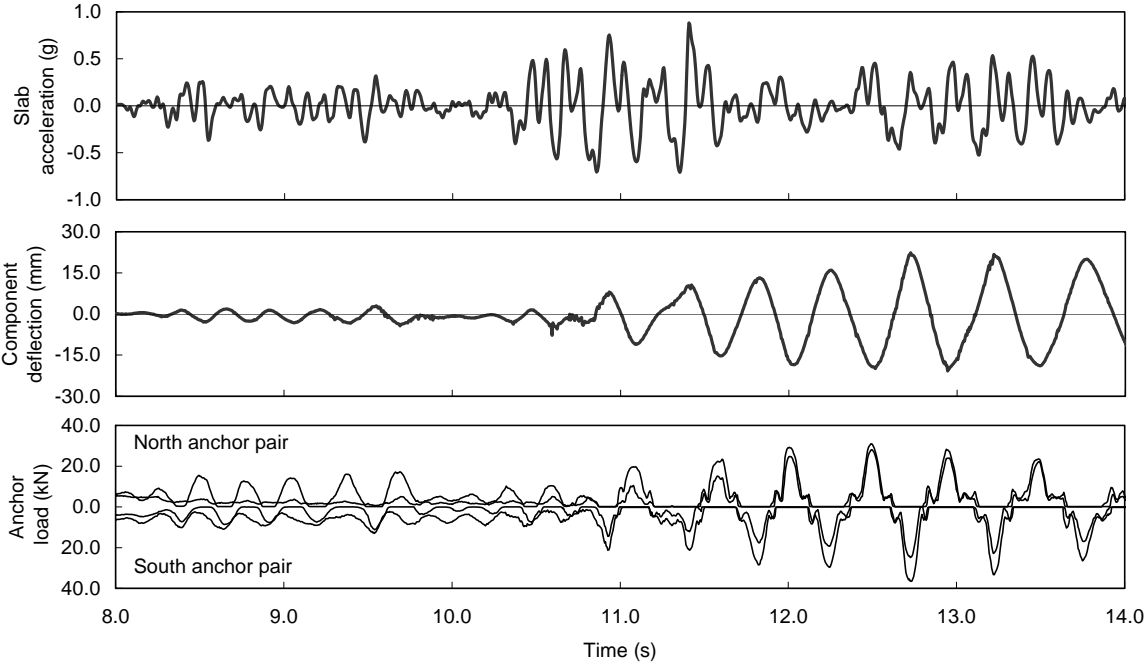


Figure 3.2. Time histories of floor acceleration, component deflection and anchor loads (example: Undercut anchor, 40% scaling)

3.2. Failure Mechanism and Ultimate Anchor Capacity

Depending on the concrete properties and the type of anchor, concrete anchors develop different failure modes. In cracked concrete, bolt-type expansion anchors typically fail in a pull-through mode. The anchor is completely pulled through the expansion elements, in which course the anchor bolt experience large displacements. Undercut anchors fail when either the concrete or steel capacity is exceeded. The larger the concrete crack, the more the concrete capacity is reduced and steel failure becomes increasingly governing.

In case of the tested undercut anchors, the north anchor pair failed simultaneously in steel before the peak acceleration of the record was reached during the test run with a scale factor of 130 % at 10.7 seconds (Fig. 3.3). In case of the tested expansion anchors, the northeast anchor pulled through after the strong motion portion of the test run with a scale factor of 60 % at 15.0 seconds (Fig. 3.4). Also the northwest anchor was clearly beyond its peak capacity at that time. The concrete remained intact and there was no concrete breakout in both cases. After failure of one anchor pair, the component was still attached to the slab by the other anchor pair. The loss of one anchor pair amidst the shaking action changed the kinematic system to a kind of pendulum and the remaining anchors had to cope with high reactive loads. The ultimate capacity of the remaining anchors was nearly exhausted and the complete failure of the component was imminent.

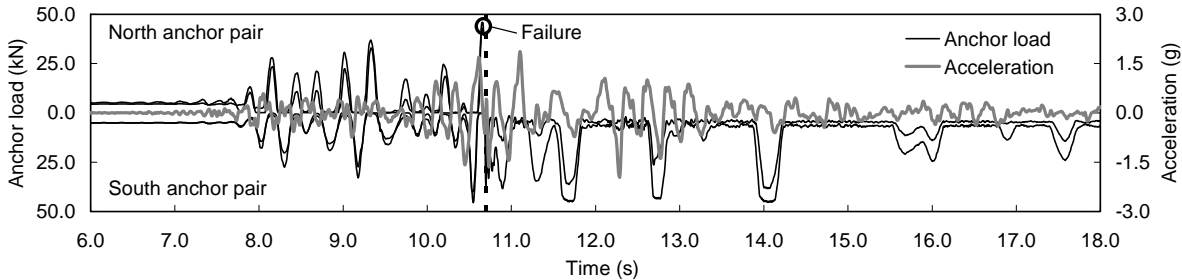


Figure 3.3. Anchor load and acceleration time histories for final failure test on undercut anchors (130 % scaling)

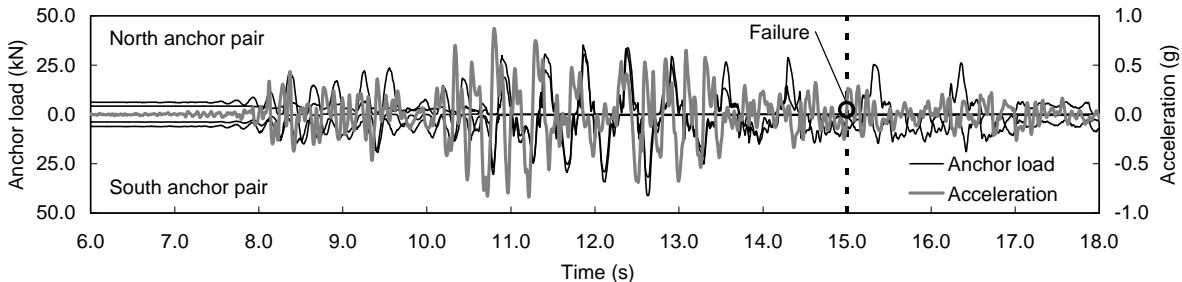


Figure 3.4. Anchor load and acceleration time histories for final failure test on expansion anchors (60 % scaling)

The dashed lines in Figs. 3.5 and 3.6 indicate the monotonic capacities derived from reference tests on single anchors in constant width cracked concrete (0.8 mm). In both cases, the load-displacement curves frequently exceeded the monotonic mean envelope for cracked concrete due to crack closure. At the moment of failure, the crack width was approximately 0.15 mm. For the undercut anchors (Fig. 3.5), the steel failure loads (43.1 kN in the northwest anchor and 45.9 kN in the northeast anchor) were significantly lower than the monotonic steel capacity of 48.9 kN, probably because of low cycle fatigue induced by bending of the bolt in the tight footing during strong model component deflections. After the failure of the north anchor pair, the south anchor pair was heavily loaded, however, made it through the remaining portion of shaking.

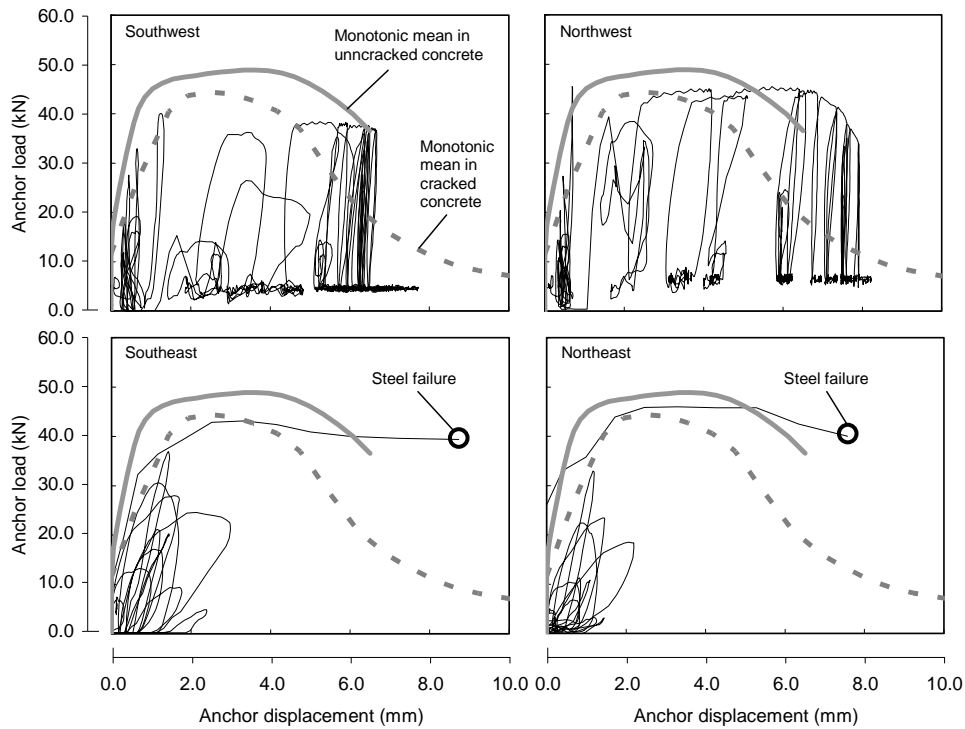


Figure 3.5. Load-displacement curves of final failure test on the undercut anchor (130 % scaling)

For the expansion anchors (Fig. 3.6), the displacements of the north anchor pair were substantially larger than that of the south anchor pair. The maximum anchor loads (35.3 kN in the northwest anchor and 33.9 kN in the northeast anchor) is within the range of the monotonic capacities in cracked and uncracked concrete. Prior to failure, the northwest anchor observed decreasing load demand, while the northeast anchor steadily increased its load carrying demand to enforce the load carried on the north side of the component. This soft transition of load avoided an abrupt overload of the remaining anchors at the moment of final failure.

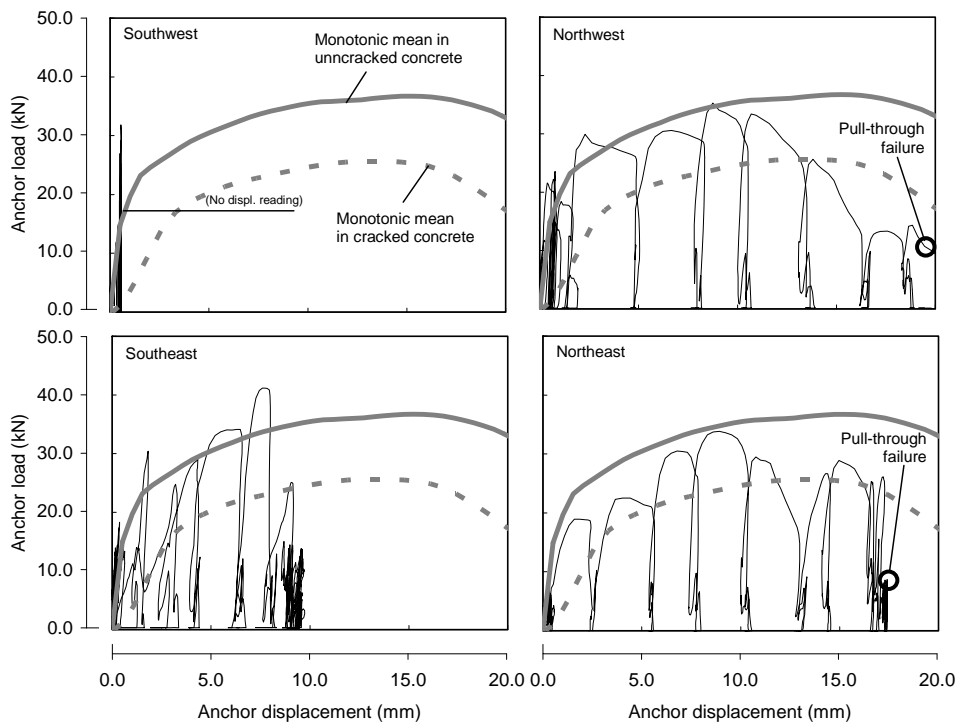


Figure 3.6. Load-displacement curves of final failure test on the expansion anchor (60 % scaling)

The diagrams in Fig. 3.7 plot the acceleration versus the drift ratio at the CoG of the component during the final test for each of the anchors tested. The drift ratio is calculated by dividing the horizontal displacement of the model component by the distance ℓ to the slab (Fig. 3.1). Displacement and acceleration are measured at the CoG. Due to larger anchor displacement capacities, the drift ratio for the expansion anchor (maximum 5%, Fig. 3.7b) is considerably larger than for the undercut anchor (maximum 2%, Fig. 3.7a).

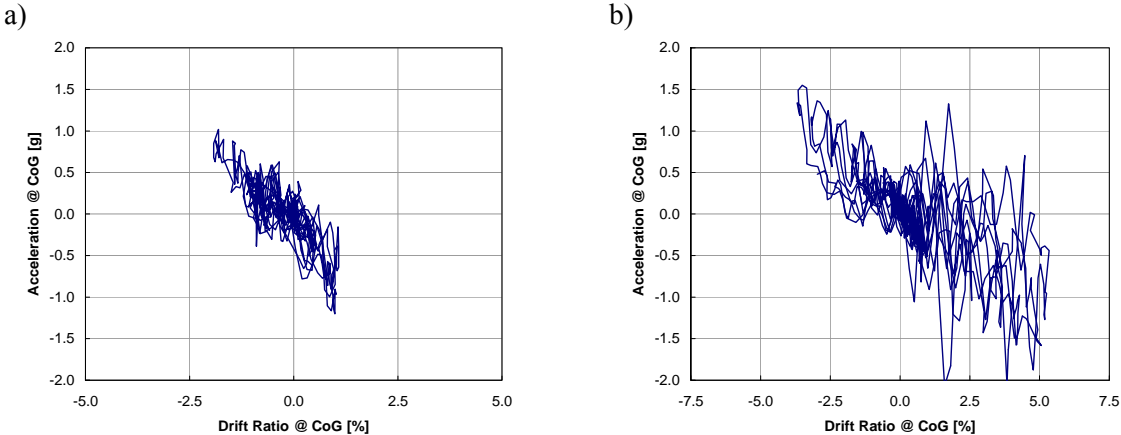


Figure 3.7. Acceleration versus drift ratio of the model component for the final failure tests on a) undercut anchor and b) expansion anchor

3.3. Effect of Anchor Load-displacement Characteristics on the Test Results

Fig. 3.8 plots the maximum anchor load and the accumulated anchor displacement as the average of all four anchors. For a given scale factor, the anchor displacements for undercut and expansion anchors are very different, but the maximum anchor load is not. Moreover, analysis of the spectral response as well as of the load time histories yielded for all tests and both anchor types a uniform elongation of the period to 0.45 seconds (exemplary shown in Fig. 3.1b). Apparently, different load-displacement characteristics of various anchor types do not influence the oscillating behaviour of the component.

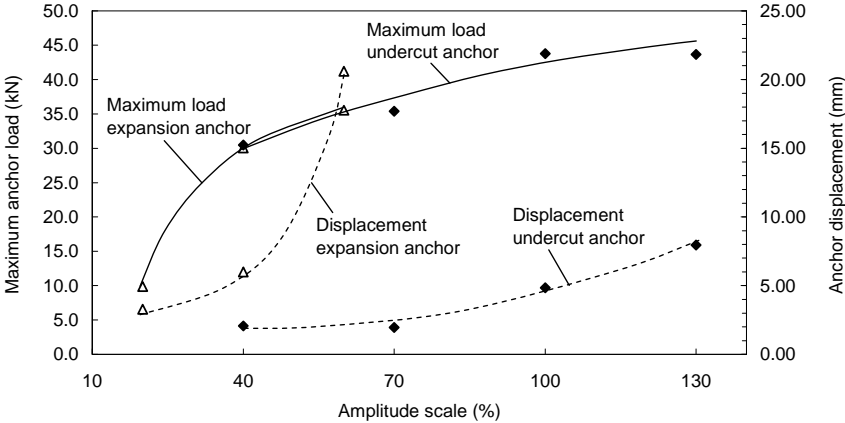


Figure 3.8. Maximum anchor load and accumulated anchor displacement versus amplitude scales (trend lines are nonlinear regressions)

Since the peak spectral acceleration of the underlying floor motion is close to 0.25 seconds, the elongation shift down the descending branch helps the component to elude the maximum amplification (Fig. 3.1b) and therefore to reduce the anchor loads. However, whether the anchor deformation capacity is beneficial or adverse, will highly depend on the specific characteristics of the component and motion spectral demand.

4. CONCLUSIONS

The shake table tests on an anchored model component in suspended configuration were the first of its kind and resulted in valuable data for investigating post-installed anchor behaviour when a suspended nonstructural component is subjected to real earthquake motions. For the simulation of the acceleration and corresponding crack behaviour in the floor segment, a complex testing infrastructure was developed. It is important to note that these tests were focused on testing the anchors to failure. No relation between the failure loads and mechanisms observed and acceptance criteria for seismic anchor qualification can be drawn from these tests.

Though gravity loads act on the connection, the load transfer system is earthquake load dominated. As the anchors respond to the cyclic actions, they displace but show a robust behaviour. By incrementally increasing the scale factor, the anchor design capacities are considerably exceeded. The eventual failure of some of the anchors leads to a near-complete failure of the anchored component. In the multi-anchored configuration of the model component here, however, redistribution of loads facilitates a system that can remain stable. The seismic demand acting on the anchors connecting components to concrete primarily depends on the spectral floor acceleration at the elongated period of the component. The load-displacement characteristics of the anchor type affect the accumulating anchor displacements, however, the effect on the maximum anchor loads during shaking is insignificant.

ACKNOWLEDGEMENT

This project was supported by the Hilti Corporation. The helpful suggestions from the project team and Oversight Committee members are appreciated. In addition to the authors, project team members include Professor Rob Dowell of San Diego State University, Dr. Derrick Watkins and Ricky Wood both of UCSD. Project Oversight Committee members include Uli Bourgund, Rainer Hüttenberger, and John Silva of Hilti, and Dean Frieder Seible of UCSD. The assistance of the Charles Lee Powell Laboratory staff – namely, Paul Greco and Andy Gundthardt – as well as undergraduate students are greatly appreciated. The opinions, findings, and conclusions expressed in this paper are those of the authors and do not necessarily reflect those of the sponsoring agency. The German Academic Exchange Service (DAAD) provided partial grant for the corresponding author. The supports are gratefully acknowledged.

REFERENCES

- ACI 355.2 (2007), Qualification of post-installed mechanical anchors in concrete (ACI 355.2-07) and commentary, American Concrete Institute (ACI), Farmington Hills, Michigan.
- ASCE 7 (2010): Minimum design loads for buildings and other structures: Revision of ANSI/ASCE 7-10, American Society of Civil Engineers (ASCE), Reston, Virginia
- Bachmann, H. (2002), Erdbebensicherung von Bauwerken (Earthquake Guarding of Buildings), 2. überarbeitete Auflage, Birkhäuser Verlag, Basel. (In German)
- Bergmeister, K. (1988), Stochastik in der Befestigungstechnik mit realistischen Einflussgrößen (Stochastic in fastening technology under realistic variables), Dissertation, Universität Innsbruck. (In German)
- Eligehausen, R., Lotze, D. and Sawade, G. (1986), Untersuchungen zur Frage der Wahrscheinlichkeit, mit der Dübel in Rissen liegen (Investigation of the probability that anchors are located in cracks). Report No. 1/20-86/17, Institut für Werkstoffe im Bauwesen, Universität Stuttgart. (In German)
- Herdman, R. (1995), Reducing Earthquake Losses, U.S. Congress, Office of Technology Assessment, OTA-ETI-623.
- Hoehler, M. (2006), Behavior and testing of fastenings to concrete for use in seismic applications, Dissertation, IWB, Universität Stuttgart.
- Paulay, T. and Priestley, N. (1992), Seismic design of reinforced concrete and masonry buildings. John Wiley & Sons, Inc.
- Schuler, D. (2007), Erdbebensicherheit von nichttragenden Bauteilen, Installationen und Einrichtungen (Earthquake resistance of nonstructural components). Tag der Befestigungstechnik, Zürich. (In German)
- Taghavi, S. and Miranda, E. (2003): Response Assessment of Nonstructural Building Elements. PEER 2003/05, Pacific Earthquake Engineering Research Center, University of California, Berkeley College of Engineering
- Watkins, D., Hutchinson, T. (2011), Seismic performance of nonstructural components anchored in concrete with cyclic cracks. SSRP-2010/07, University of California, San Diego.
- Wood, R., Hutchinson, T. and Hoehler, M. (2010), Cyclic load and crack protocols for anchored nonstructural components and systems. SSRP-2009/12, University of California, San Diego.